

# MARKOV POINT PROCESS: 3D VORONOI TESSELLATIONS GENERATED BY STRAUSS PROCESS

KAREL BODLÁK, PETR PONÍŽIL AND IVAN SAXL

ABSTRACT. The mutual arrangement of points constituting independent realizations of the conditional and unconditional Strauss process with variable parameters  $R, \gamma$  is characterized by the properties of Voronoi tessellations generated by examined point patterns.

Абстракт. Взаимное расположение точек, составляющих независимые реализации условного и безусловного Штраусовского процесса с переменными параметрами  $R, \gamma$  характеризуется свойствами мозаик Воронова генерированных на основе исследуемых точечных моделей.

## 1. INTRODUCTION

The Gibbs point processes [13] describe very large systems in the theories of statistical physics, *e.g.* mutual behaviour and arrangement of particles in some material at different temperatures. First we consider processes with a fixed number of points. Let data be represented by a finite point configuration  $x = \{x_1, \dots, x_n\}$  in some bounded subset  $B$  of the  $d$ -dimensional Euclidean space. The used form of the probability density function with respect to the Lebesgue measure  $\mu$  is

$$(1) \quad f_n(x) = \frac{1}{Z} \exp(-U(x)),$$

where  $Z$  is a normalizing constant,  $U$  is the energy function. Usually  $U$  is of a special form

$$U(x) = \sum_{1 \leq i < j \leq n} \theta(\|x_i - x_j\|).$$

The function  $\theta$  is called the pair potential and describes attractive and repulsion forces depending on inter-point distances.

The general form of a density of Markov point processes [12, 13] according to the Hammersley-Clifford theorem is of the form (1) [4]. Hence all Markov point processes are Gibbs point processes. We assume a special case of the pair potential  $\theta(r)$  in this work ( $b > 0, \rho > 0$ ):

$$\theta(r) = \begin{cases} \infty, & r = 0 \\ b, & 0 < r \leq \rho \\ 0, & r > \rho. \end{cases}$$

---

2000 *Mathematics Subject Classification.* Primary 60J99; Secondary 62M30.

*Key words and phrases.* Strauss process, Voronoi tessellations, point patterns.

The research was supported by Grant No. 201/99/0269 of GA ČR (K.B., I.S.), by the Ministry of Education of the Czech Republic (contract No. VS96108 - P.P.) and by Grant No. 304/00/1622 of GA ČR (I.S.).

We obtain the specific Markov point process which is called the Strauss point process [12, 13, 15]. Its density is

$$(2) \quad f_n(x) = \frac{1}{Z} \exp(-bs(x)), \quad \rho > 0,$$

where  $s(x)$  is the number of point pairs the Euclidean distance of which is less than  $\rho$ . Substituting  $\gamma = \exp(-b)$ , then  $\gamma \in (0, 1)$  and the density (2) has the form

$$(3) \quad f_n(x) = \frac{1}{Z} \gamma^{s(x)}.$$

An elegant approach to a random number of points consists in considering the measurable space  $(N, \mathcal{N})$  of finite sets of distinct points in  $B$ , - see [4]. Then the Strauss point process has a density with respect to the distribution of a Poisson point process with the finite intensity measure  $\mu$  given by

$$(4) \quad f(y) = \alpha \beta^{n(y)} \gamma^{s(y)}, \quad y \in N,$$

where  $\alpha$  is a normalization constant,  $\beta > 0$  and  $\gamma \in (0, 1)$  are parameters,  $n(y)$  is number of points.  $\gamma = 1$  gives a Poisson point process with intensity measure  $\beta\mu$ . The parameter  $\gamma = 0$  conditionally on no point pair being closer than  $\rho$  produces a hard-core process. For  $\gamma \in (0, 1)$ , there is a repulsion between the points which increases as  $\gamma$  decreases ( $b$  is greater). The density (4) is not integrable for  $\gamma > 1$ .

The simulation studies of 2D Strauss process [1, 3, 4, 5] have shown the results as follows. Patterns of a conditional model (fixed number of points  $n$ , called also the canonical ensemble in analogy to statistical physics) show regularity at  $R = 0.35$  (after renormalizing  $\rho$  to the unit point intensity:  $R = \rho n^{1/2}$ ) not only at  $\gamma = 0.02$  but also at  $\gamma = 0.5$  whereas at  $R = 1.76$  clustering is pronounced at  $\gamma = 0.05$  as well as at  $\gamma = 0.02$  but the pattern of clusters is quasi-regular in the latter case [4] ( $n = 50$  in a unit square). The clustering at  $\gamma > 1$  is studied in [3] ( $n = 100$  in the unit square,  $R = 1$ ,  $\gamma = 2$ ): an equilibrium state with few clusters and small number of isolated points was attained already after 200 iterations. As demonstrated by [1], the transition from the complete spatial randomness (binomial-like process) to clustering is abrupt without intermediate moderately clustered patterns. On the other hand, in contrast to hard-core processes of the Matérn type II and SSI (simple sequential inhibition), Strauss process at  $\gamma = 0$  produces highly regular point patterns with the packing densities (the area fraction of non-overlapping discs of radius  $R$  centred in the points of the pattern) close to the theoretical values [5].

The process with random number of points (unconditional process, grand canonical ensemble) is less suitable for the analysis carried out in the present paper because cluster states cannot be attained by the used MCMC algorithm. A detailed investigation of this case is described in [2].

The methods used in the above papers include visual inspection, estimation of  $n(x)$ ,  $s(x)$ , second- and third-order characteristics (the pair-correlation function, alignment function) and hexagonality number (the probability that a disk of radius  $r \gtrsim R$  centred at a typical point  $x$  contains exactly 6 other points like in the close-packed arrangement of disks). There are no published papers on 3D Strauss model as yet, at least as far as the knowledge of the authors goes.

Here another approach is chosen, namely the analysis of the Voronoi tessellation generated by the examined point processes (a similar qualitative analysis was used in [3] for the 2D nearest-neighbour Markov point process). Because of the one-to-one correspondence between the generating point process and the tessellation, its

geometric characteristics sensitively reflect the spatial arrangement of the process. The standard goal of such an analysis concerns (i.) degree of the regularity of the pattern (translation lattices produce isohedral tilings, which are more or less distorted if generating patterns are displaced lattices of the Bookstein model type - [8]), (ii.) hard- or soft-core property (Matérn hard-core processes, process of the simple sequential inhibition - SSI, Strauss process, (iii.) mutual independence of the point positions (stationary Poisson point process), (iv.) tendency to clustering (Neyman-Scott processes [13], Bernoulli cluster fields [11]). In order to recognize the basic rule governing analyzed point pattern, it is sufficient to consider the unit tessellations only, which means that a point pattern is renormalized to the unit intensity  $\lambda = 1$ ; then also the mean cell volume  $\mathbf{E}v = 1/\lambda = 1$  and  $R = \rho(\mathbf{E}n)^{1/3}$ . The cell volume variance  $\text{var } v$  (or, equivalently, CV  $v$ ) is a sensitive characteristic of the point arrangement and its estimation is the primary step of the analysis. In the sequence of the above mentioned cases,  $\text{var } v$  increases from zero (isohedral tilings) to 0.178 (Poisson-Voronoi tessellation - PVT) and attains typically the values between 1 and 100 for various tessellation generating cluster fields.

Further information is acquired by estimating other cell properties, like are cell surface area  $s$ , cell mean breadth  $w$ , shape factors  $g = 6\sqrt{\pi}v/s^{3/2}$  (related to the isoperimetric inequality:  $g = 1$  for a sphere) and  $f = 6v/\pi w^3$  (related to the Bierbach inequality; again  $f = 1$  for a sphere), number of cell faces  $n_f$  and in particular its variance  $\text{var } n_f$ , dihedral angles *etc.*

Even when the size characteristics of any cell are mutually independent, there is a certain degree of correlation between their statistical characteristics. In particular, if only hard-, soft- and pseudo-hard-core processes are considered, then  $\mathbf{E}s$ ,  $\mathbf{E}w$ ,  $\text{var } n_f$  are approximately increasing and shape factors  $g$ ,  $f$  approximately decreasing functions of  $\text{var } v$ , resp. - see Tab. 1. Small local extremes occur near the bounds represented by tilings generated by tightly packed body centred (tetrakaidecahedrons) and face centred (rhombic dodecahedrons) cubic lattices and PVT [7]; simple cubic tessellation behaves rather exceptionally - see Fig. 4. Some cell characteristics have discontinuity at  $\text{var } v \rightarrow 0_+$  (*e.g.*  $n_f$ ).

Table 1. Cell characteristics of unit 3D Voronoi tessellations

	tetrakai-decahedron	SSI ( $R=0.82$ )	PVT	Cluster field tessellations
$\text{var } v$	0	0.019	0.178	< 100
$\mathbf{E}w$	1.34	1.40	1.46	> 0.3
$\text{var } n_f$	0	3.54	11.1	< 100
$\mathbf{E}g$	0.87	0.80	0.73	> 0.4

## 2. SIMULATION

First the examined Strauss process was simulated by means of the Markov chain Monte Carlo (MCMC) technique. The idea of MCMC is as follows: let  $X$  be a finite point process with distribution  $Q$ . In order to generate samples of it a chain is constructed of point processes  $X_0 \sim Q_0, X_1 \sim Q_1, \dots$  all on the same space such that  $\lim_{t \rightarrow \infty} Q_t = Q$  weakly and it is assumed that  $X_n$  follows approximately the given equilibrium distribution  $Q$  for  $n$  large enough.

The Metropolis-Hastings algorithm is perhaps the most widely used tool for constructing Markov chains. Both the fixed and random number cases [4] were treated.

In the conditional Strauss process with  $n(x) = k$ , tightly clustered and regularly arranged patterns are formed for  $\gamma > 0$  small and  $\rho$  exceeding certain value depending on  $k$ . For the unconditional Strauss process when  $\beta$  is large and  $\gamma$  is small (the number of points is large and the repulsion is great), the Metropolis-Hastings algorithm is inefficient: the attained number  $\mathbf{E}n$  has an upper bound  $\beta$  and decreases with diminishing  $\gamma$  - see Tab. 3.

Table 2. Effect of variables  $R$ ,  $\gamma$  on the selected unit tessellation characteristics: conditional Strauss process

R	$\gamma$	0.01	0.02	0.05	0.10	0.20	0.50	0.70	0.95
0.288	var $v$		0.160						
	$\mathbf{E}w$		1.46						
	var $n_f$		10.3						
	$\mathbf{E}g$		0.73						
0.4–0.7				)*		)*	)*		)*
0.72	var $v$	0.045	0.047	0.055		0.076	0.11		
	$\mathbf{E}w$	1.425	1.427	1.43		1.439	1.45		
	var $n_f$	5.41	5.54	5.94		7.09	8.66		
	$\mathbf{E}g$	0.79	0.78	0.77		0.76	0.74		
0.865	var $v$	0.035	0.039		0.055	0.066			
	$\mathbf{E}w$	1.411	1.415		1.43	1.44			
	var $n_f$	4.41	4.71		5.86	6.58			
	$\mathbf{E}g$	0.79	0.79		0.77	0.77			
1.01	var $v$		0.056						
	$\mathbf{E}w$		1.437						
	var $n_f$		5.52						
	$\mathbf{E}g$		0.76						
1.44	var $v$		0.213			0.20	0.12	0.105	
	$\mathbf{E}w$		1.49			1.49	1.49	1.47	
	var $n_f$		16.3			15.7	11.5	10.4	
	$\mathbf{E}g$		0.68			0.68	0.71	0.72	
2.88	var $v$		2.15				2.19	2.05	0.18
	$\mathbf{E}w$		1.23				1.24	1.24	1.46
	var $n_f$		26.3				25.7	26.5	11.6
	$\mathbf{E}g$		0.61				0.61	0.62	0.73

)\* examined range of unconditional Strauss process - see Tab. 3

The second step consisted in construction of the tessellation by means of the incremental method with the nearest neighbour algorithm [6]. Edge effects have been carefully removed by wide protecting layer (*e.g.* only  $\approx 1000$  cells remained for the examination at  $k = 3000$  in the conditional case). In the unconditional case ( $\beta = 3000$ ), the attained number  $\mathbf{E}n$ , hence also the value of  $R$  at constant  $\rho$ , varied - see Tab. 3. The number of independent realizations ranged from 100 to 1000.

Main cell characteristics have been then determined by a direct calculation and their moments about the origin  $\mu'_i(\bullet)$ ,  $i = 1, 2, 3, 4$ , estimated.

### 3. RESULTS

The obtained results are presented in the Tab. 2 for the conditional Strauss process and in Tab. 3 for the unconditional Strauss process. Only insufficient results have been obtained in the latter case, as the attained number of points produced in

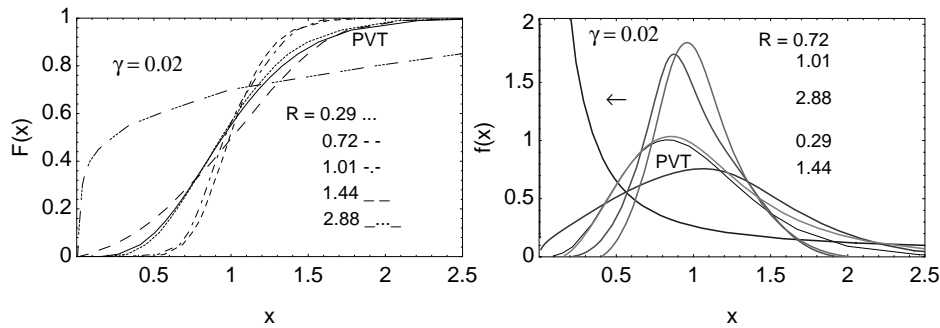


FIGURE 1. Distribution functions  $F(x)$  and probability density functions  $f(x)$  of the cell volume  $v$  at  $\gamma = 0.02$  and variable  $R$  (note the high ordering at  $R = 0.72$  and a heavy clustering at  $R = 2.88$ ).

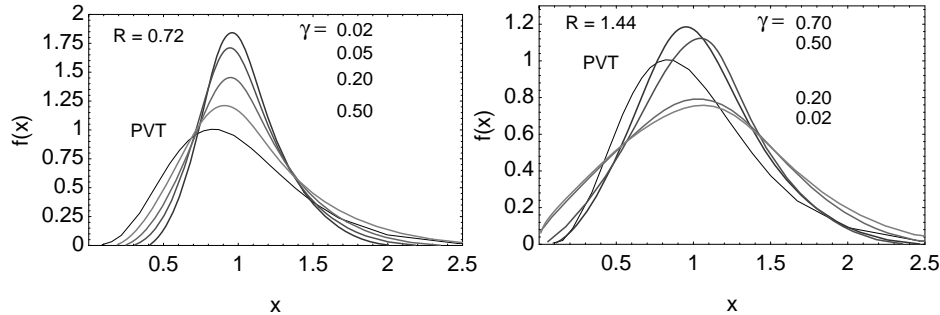


FIGURE 2. Probability density functions  $f(x)$  of the cell volume (note gradually vanishing Poisson clusters with decreasing  $\gamma$  at  $R = 0.72$  and gradually increasing amount of clustering with decreasing  $\gamma$  at  $R = 1.44$ ).

the unit cube at a selected value of the parameter  $\rho$  decreased considerably with decreasing value of  $\gamma$ .

Table 3. Effect of variables  $R, \gamma$  on the selected unit tessellation characteristics unconditional Strauss process at  $\rho = 0.05$  and  $\beta = 3000$

$\gamma$	0.05	0.20	0.50	0.95
$R$	0.43	0.46	0.50	0.70
$\mathbf{E}n$	627	755	1105	2790
var $v$	0.07	0.085	0.108	0.152
$\mathbf{E}w$	1.44	1.44	1.45	1.44
var $n_f$	6.84	7.46	8.59	10.7
$\mathbf{E}g$	0.77	0.76	0.75	0.76

#### 4. DISCUSSION OF RESULTS

##### A) Conditional Strauss process

*Effect of variable parameter  $R$  at a small interaction parameter  $\gamma (= 0.01, 0.02)$ :* the tessellation does not differ substantially from PVT at  $R < 0.3$ , a considerable ordering (var  $v < 0.1$ ) takes place at  $0.72 \leq R \leq 1.01$ , the amount of Poisson clusters decreases along the sequence  $R = 0.29 \rightarrow 0.72 \rightarrow 0.865$  and then again increases

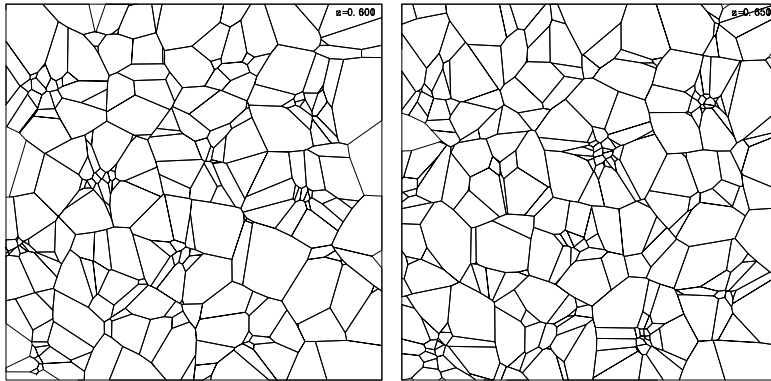


FIGURE 3. Examples of planar sections of 3D tessellations generated by the conditional Strauss process with  $R = 2.88$ ,  $\gamma = 0.5$ .

with growing  $R$ ; note the corresponding shifts of the modes and variable weights of tails in Fig. 1. A tight clustering with the mode near  $v \rightarrow 0_+$  is observed at  $R = 2.88$ .

*Effect of variable interaction parameter  $\gamma$  at a medium value of the parameter  $R(= 0.72, 0.865)$ :* the value of 0.72 is already above the value of 0.554 of the mean nearest neighbour distance  $\rho_{PVT}$  in the stationary Poisson point process. The repulsion is pronounced at  $\gamma \leq 0.2$  and still observable at  $\gamma = 0.5$ . At  $0.01 \leq \gamma \leq 0.02$ , the values of  $\text{var } v$  and  $\text{var } n_f$  are already lower than the corresponding values attainable in the tessellations generated by the Matérn type II process [7]. The shifts of the mode and the symmetrization of the cell volume probability density function are clearly perceptible, the both tails of the cell volume distributions are the lighter the smaller is  $\gamma$  - see Fig. 2. The equivalent diameter of the observed minimum cell in the samples (of the size  $10^5$  cells)  $R_{min} = (6v_{min}/\pi)^{1/3}$  decreases from 0.85 ( $\gamma = 0.02$ , a strong repulsion) to 0.61 ( $\gamma = 0.50$ , a mild repulsion) in a rough agreement with the actual values of the parameter  $R$ .

*Effect of variable interaction parameter  $\gamma$  at high values of  $R$ :* A very similar tight clustering takes place at all but one (0.95) values of  $\gamma$  at  $R = 2.88$ , all characteristics are nearly the same in the broad examined range  $[0.02, 0.7]$ , which is rather surprising. The equivalent diameter  $R_{min}$  is of the order of 0.1 only, whereas the value of 0.5 can be expected for PVT and a sample of similar size. At  $R = 1.44$ , the amount of clustering is much less pronounced, however, it distinctly decreases with growing  $\gamma$ . In contrast to the case of medium and small values of  $R$ , the both tails of the cell volume distributions are the heavier the smaller is  $\gamma$  - Fig. 2. A similar value of  $\text{var } v$  describes tessellations generated by Neyman-Scott process of Matérn clusters with the daughter number  $N = 20$  and the ball diameter  $R < 0.2\rho_{PVT}$ . However, the quasi-regularity of cluster arrangement observable in 2D sections and number of hit small inner cells indicate that a comparison with tessellations generated by lattice cluster fields is more correct - then the estimate  $N \approx 50$  would be more realistic [8, 9, 10]. The ordering of clusters is then similar as in the 2D case [4].

#### B) Unconditional Strauss process

The results can be incorporated into Tab. 2 – the row with \*)\* – and then they do not differ substantially from the values obtained for the conditional Strauss process (see also Fig. 4). The obtained tessellations roughly correspond to the tessellations

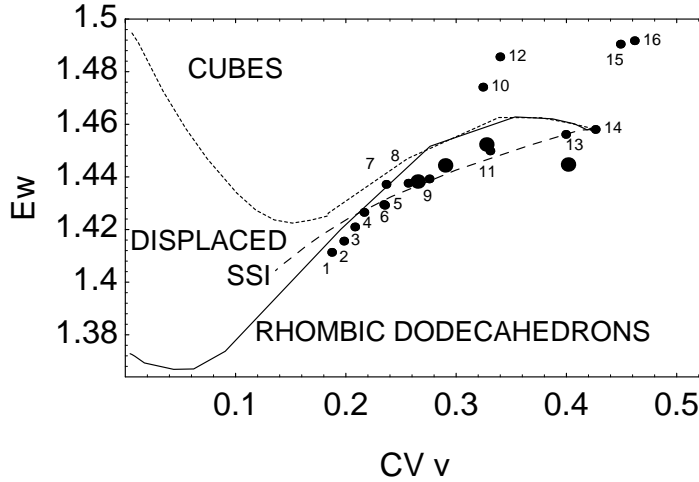


FIGURE 4. Mean widths of tessellations generated by displaced cubic simple and face centred cubic lattices, by the process of simple sequential inhibition (SSI) [7] and by examined cases of Strauss process (small numbered points - conditional process; great points - unconditional process); the tightly clustered cases 17–19 have been omitted (for explanation of low  $\mathbf{E}w$  see [9]). The values of  $\gamma$ ,  $R$  corresponding to the numbers in the plot are shown in the Tab. 5.

generated by the Matérn type II process [7] (Tab. 4). They may also be compared with the 2D simulation using Metropolis-Hastings algorithm [2]: at  $\gamma = 0.75$ ,  $\rho = 0.1$  and  $\beta = 100$  in a unit square, the mean number of points  $\mathbf{E}n \approx 65 = 0.66\beta$  was attained. Renormalizing to a unit mean intensity,  $R = \rho\sqrt{\mathbf{E}n} \approx 0.1 \times 8.1 = 0.81$  and not 1 as expected. Similarly in Tab. 3: by interpolation between  $\gamma = 0.5$  and  $0.95$ , the gain of points  $1950/\beta$  is also  $\approx 66\%$  at  $\gamma = 0.73$  and  $R = 0.62$ .

Table 4. Selected characteristics of the unit tessellation generated by the 3D Matérn type II process

$R$	0.62	0.52	0.380	PVT
var $v$	0.057	0.088	0.134	0.178
$\mathbf{E}w$	1.43	1.44	1.45	1.46
var $n_f$	6.09	7.59	9.41	11.1
$\mathbf{E}g$	0.77	0.77	0.74	0.73

### C) Conclusions

It can be concluded that if  $R$  is high ( $\geq 5\rho_{PVT}$ ) clustering persists even at rather high values of  $\gamma$  ( $\approx 0.7$ ) and a dissolution of clusters takes place only at  $\gamma$  as high as 0.95. At  $R \approx 2.6\rho_{PVT}$ , clustering is distinct only at low values of  $\gamma$ , whereas partial order is established at higher values of  $\gamma$  and vanishes again at  $\gamma \rightarrow 1$ . Only at sufficiently low  $R$ , the degree of the order is inversely proportional to  $\gamma$ . On the other hand, ordering is poor even at small values of  $\gamma$  if  $R$  is low ( $\leq 0.5\rho_{PVT}$ ). The results are comparable with the qualitative 2D results [4].

Table 5 Survey of examined cases (conditional Strauss process) - see Fig. 4

$R \setminus \gamma$	0.01	0.02	0.05	0.10	0.20	0.50	0.70	0.95
0.288		13						
0.72	3	4	5		9	11		
0.865	1	2		6	8			
1.01		7						
1.44		16			15	12	10	
2.88		18				19	17	14

Mean width  $\mathbf{E}w$  together with CV  $v$  are two suitable characteristics of any tessellation; the comparison of  $\mathbf{E}w$  vs CV  $v$  plots of tessellations generated by selected hard- and pseudo-hard-core processes with the values obtained in the present pilot study classifies the examined cases of the Strauss process in the broader framework. Clearly, lower values of  $\gamma$  and perhaps slightly higher values of  $R$  should be selected in order to obtain more regular point pattern and, consequently, a tessellation approaching isohedral tilings of the dodecahedral or tetrakaidecahedral types.

## REFERENCES

- [1] GEYER, C.J., THOMPSON E.A.: Annealing Markov Chain Monte Carlo with Application to Ancestral Inference Analysis. *J. Amer. Statist. Assoc.* **90** (1995), 909-920.
- [2] GEYER, C.J., MØLLER J.: Simulation Procedures and Likelihood Inference for Spatial Point Processes. *Scand. J. Stat.* **21** (1994), 359-373.
- [3] MØLLER J.: Extensions of the Swendsen-Wang Algorithm for Simulating Spatial Point Processes. Research Report no.246, University of Aalborg, Aalborg 1992.
- [4] MØLLER J.: Markov Chain Monte Carlo and Spatial Point Processes. In: *Stochastic Geometry: Likelihood and Computation* (O.E. BARNDORFF-NIELSEN, W.S. KENDALL, M.N.M. VAN LIESHOUT, EDS.). Chapman and Hall, London 1999, p. 141-172.
- [5] MASE S., MØLLER J., STOYAN D., WAAGEPETERSEN R.P., DÖGE G.: Packing Densities and Simulated Tempering for Hard Core Gibbs Point Processes. Research Report R-99-2002, University of Aalborg, Aalborg 1999.
- [6] OKABE A., BOOTS B., SUGIHARA K.: Spatial Tessellations. J. Wiley & Sons, Chichester 1992.
- [7] PONÍŽIL P. AND SAXL I.: Properties of 3D Poisson hard-core and pseudo-hard-core fields II. Voronoi tessellations. In: *Proc. S<sup>4</sup>G, Int. Conf. on Stereology, Spatial Statistics and Stochastic Geometry*, (V. Beneš, J. Janáček and I. Saxl, eds.). JČMF, Praha 1999, p. 227-239. See also a substantial part of all data and a summarizing paper on the Internet address: <http://fyzika.zlin.vutbr.cz/voronoi/>.
- [8] SAXL I.: Analýza náhodných bodových vzdáleností a Voronoiovy teselace systémů. In: *Robust'98* (Antoch J. & Dohnal G., eds.). JČMF, Praha 1998, p. 161-178.
- [9] SAXL I. AND PONÍŽIL P.: 3D Voronoi tessellations of cluster fields. *Acta Stereol.* **17** (1998), 237-246.
- [10] SAXL I. AND PONÍŽIL P.: 3D Voronoi tessellations generated by Poisson and lattice cluster fields. *Acta Stereol.* **17** (1998) 247-252.
- [11] SAXL I., SÜLLEIOVÁ K., PONÍŽIL P.: 3D Simulations of intergranular fracture. In: *Proc. Int. Conf. "Fractography 2000"*, (Parilák L., ed.). Vysoké Tatry, 15 - 18. 10. 2000. ÚMV SAV, Košice 2000, p. 94-107.
- [12] SØRENSEN DAM T., THOMSEN B. J.: *Spatial Point Processes* (A Master of Science Thesis in Statistics). University of Aalborg, Aalborg 1999.
- [13] STOYAN D., KENDALL W. S. AND MECKE J.: *Stochastic Geometry and its Applications*. J. Wiley & Sons, New York 1995.
- [14] STOYAN D., STOYAN H.: *Fractals, Random Shapes and Point Fields*. J. Wiley & Sons, New York 1994.
- [15] STRAUSS D. J.: A model for clustering. *Biometrika* **63** (1975), 467-475.

*E-mail address:* bodlak@karlin.mff.cuni.cz, saxl@math.cas.cz, ponizil@math.cas.cz